LIMNOLOGY and OCEANOGRAPHY LETTERS

ASLO

Open Access

Limnology and Oceanography Letters 11, 2026, e70172

doi: 10.1002/lol2.70172

LETTER

A dual role of phycoerythrin in the nitrogen-fixing cyanobacterium *Crocosphaera watsonii*: From light-harvesting to nitrogen reservoir

Takako Masuda [1a*] **Grzegorz Konert** [1b] **Dominik Pinkas** [2] **Marie Vancová** [3] **Vlada Filimonenko** [2] **Radek Kaňa** [1] **Ondřej Prásil** [1]

[1]Institute of Microbiology, The Czech Academy of Sciences, Třeboň, Czechia; [2]Institute of Molecular Genetics, The Czech Academy of Sciences, Prague, Czechia; [3]Institute of Parasitology, The Czech Academy of Sciences, Biology Centre, České Budějovice, Czechia

Scientific Significance Statement

Crocosphaera watsonii is a widespread unicellular cyanobacterium that contributes substantially to marine nitrogen fixation. However, its populations display heterogeneous nitrogen fixation activity under stress, with only a subset of cells actively fixing nitrogen at any given time. The mechanisms underlying cellular-level variability remain unclear. In this study, we present evidence that the structural state and intracellular localization of phycoerythrin, a pigment-protein complex traditionally regarded as a light-harvesting component, are associated with nitrogen fixation activity. These findings suggest an alternative functional role for phycoerythrin as a dynamic intracellular nitrogen reservoir. This dual role offers a mechanistic explanation for the observed heterogeneity in nitrogen fixation and provides new insight into how marine diazotrophs coordinate photosynthesis and nitrogen metabolism.

Abstract

Unicellular diazotrophic cyanobacteria contribute up to ~50% of marine N_2 fixation, and *Crocosphaera watsonii*, characterized by high phycoerythrin (PE) content, is among one of the key species in tropical and subtropical oceans. Although recent observations have revealed heterogeneous N_2 fixation activity within *C. watsonii* populations, the mechanisms behind its heterogeneity remain unresolved. Here, we hypothesize that PE's structural state is associated with the regulation of N_2 fixation. Using single-cell fluorescence spectroscopy, we observed that photosystem-uncoupled free PE was exclusively present under diazotrophic conditions and localized to the central cytoplasmic region. While mean PE fluorescence remained unchanged, PE : allophycocyanin ratios declined at the periphery in the night. These findings suggest an additional role for PE, potentially as a temporary nitrogen reservoir to buffer cellular N levels during active N_2 fixation, beyond its established light-harvesting function.

*Correspondence: takakomasuda.fra@gmail.com, takakom@fra.go.jp

[a]Present address: Fisheries Resources Institute, Japan Fisheries Research and Education Agency, Shiogama, Miyagi, Japan
[b]Present address: Department of Life Technologies, University of Turku, Turku, Finland

Associate editor: Xianhui Wan

Marine N_2 fixation provides ~100–150 Tg N annually, nearly half of global biological N_2 fixation. Up to half of this occurs in aquatic environments and is driven largely by unicellular diazotrophs (Montoya et al. 2004; Gruber and Galloway 2008). However, nitrogenase—the key enzyme for N_2 fixation—is irreversibly inactivated by O_2, posing a fundamental challenge for autotrophic cyanobacteria depend on harvesting energy and reductant power from oxygenic photosynthesis. To overcome this conflict, cyanobacteria employ strategies such as spatial segregation (heterocysts in multicellular forms) or temporal separation of processes. Unicellular cyanobacteria, including *Crocosphaera watsonii*, typically fix N_2 at night, when O_2 evolved from photosynthesis is absent.

Crocosphaera watsonii (3–8 μm in diameter) is an abundant diazotroph distributed across tropical and subtropical oceans (Masuda et al. 2024). Like other unicellular diazotrophic cyanobacteria, it performs oxygenic photosynthesis during the day, generates cellular energy and reductant power, and shifts N_2 fixation to the night period to avoid oxygen-mediated inactivation of nitrogenase (Shi et al. 2010; Dron et al. 2012). Field and culture studies have revealed that not all cells in a population actively fix N_2 (Foster et al. 2013; Mohr et al. 2013; Masuda et al. 2020). This phenotypic heterogeneity may reflect an energy-saving strategy, allowing a subset of cells to support others and thereby broaden ecological niche (Masuda et al. 2020). While high O_2 and dissolved nitrogen (i.e., ammonium) are known as inhibitors of N_2 fixation (Montoya et al. 2004; Mulholland et al. 2004), the mechanism underlying this heterogeneity remains unclear.

One of the most prominent traits of *C. watsonii* is its high cellular content of phycoerythrin (PE), which imparts its characteristic yellow-green color (Zehr et al. 2001). This pigment abundance initially led to its identification as a "PE containing nano-sized diazotroph," later classified as *C. watsonii* WH8501 (Swanson et al. 1991). Since then, multiple *C. watsonii* strains have been isolated from tropical and subtropical oceans (Zehr et al. 1998, 2001; Neveux et al. 1999). PE in *C. watsonii* is notable for its high phycourobilin (PUB) content, which, alongside phycoerythrobilin (PEB), enables efficient absorption of blue (~500 nm) and green (~565 nm) light (Fujita and Shimura 1974)– a key adaptation for light harvesting in oligotrophic, blue-light dominated marine environments. Under optimum conditions, phycobilisomes (PBS) can account for ~50% of the total soluble protein, with PE accounting for up to 20% of cellular protein (Rodriguez et al. 1989). The PE-to-chlorophyll (Chl) ratio is estimated at ~20, fivefold higher than in *Trichodesmium*, a multicellular oceanic diazotroph (Bell and Fu 2005). Previous studies have reported heterogeneous PE allocation based on the cellular fluorescence (Masuda et al. 2022, 2024), yet the underlying causes and implications of this variability remain unexplored. Given earlier reports linking PE to nitrogen storage in cyanobacteria (Wyman et al. 1985), we hypothesized that both the abundance and structural state of PE may be mechanistically linked to N_2 fixation regulation in *C. watsonii*.

Methods

Strain, cultivation and experimental conditions

We used the *Crocosphaera watsonii* PS0609, isolated initially from Philippine Sea (Masuda et al. 2013); later its *nif*H sequence was used as standard clone for Group B (AB928305) in (Shiozaki et al. 2014) (hereafter *C. watsonii*) maintained in YBC-II medium without any combined nitrogen source (Chen et al. 1996) at 28°C. Light irradiance followed a 12 : 12, light : dark cycle with 50 μmol photons m^{-2} s^{-1} irradiance in Erlenmeyer flasks. To examine the effect of light intensity, a condition with light intensity at 100 μmol photons m^{-2} s^{-1} was prepared. For the experiment, the stock culture was diluted to 1×10^6 cells mL every week more than three times, and the confocal observations were conducted 3 d after the dilution. The ammonium condition (50 μM NH_4^+ enriched medium) was prepared to examine the effect of nitrogen source, and cells were acclimated for more than three generations. Cell growth was monitored by cell counts using Coulter Counter (Beckman, Multisizer 4, United States).

Physiological measurements

Growth rate, Chl *a* per cell, POC/PON, and N_2 fixation rate were measured under diazotrophic and ammonium-replete (50 μM NH_4Cl, daily) conditions, in triplicate ($n = 3$). Growth rate was determined from Coulter Counter cell counts during exponential growth; Chl *a* per cell followed (Porra et al. 1989). POC/PON were measured on pre-combusted GF/F filters using an elemental analyzer (PE2400, PerkinElmer, U.S.A.). N_2 fixation was estimated by acetylene reduction (10% v/v, 1 h; gas chromatograph Trace 1300, Thermo Fisher Scientific, Italy) and a 4 : 1 ($C_2H_4 : N_2$) conversion factor (Montoya et al. 1996). One replicate (12D, –N) was excluded as an outlier (C : N ratio > 2 SD from the mean).

Confocal microscopy analysis and image processing

We acquired images using Laser Scanning Microscope LSM880 (Zeiss, Germany) with the Plan-Apochromat 63/1.4 Oil DIC M27 objective. Live *C. watsonii* cells were imaged in three channels corresponding to: (1) PC excited PBS (excited at 633 nm; emission detected at 641–677 nm); (2) Chl and PUB excited PE (excited at 488 nm; emission detected at 490–606 nm); (3) Chl and PUB excited Chl (exited at 488 nm; emission detected at 695–758 nm). We note that Chl emission is used to detect PSII in this study. Different allocation between (1) and (2) shows the disconnection of PE from PBS, and different allocation between (1) and (3) shows PBS disconnected from PSII in the thylakoid membrane. Secondly, we performed lambda scans from 410 to 495 nm in 9 nm intervals in 32 steps with excitation at 488 nm. The collected images (8 bit; 512 × 512; 8.24 μs dwell time; 1 Airy unit pinhole) were processed in ImageJ (FIJI distribution) using the

macro "Crocosphaera_extraction.txt" with steps explained on https://github.com/gekoneCAC/Crocophaera-extraction.

Statistical analysis

Statistical analyses were performed using Python (version 3.12.2). Cells showing segmentation failure or undergoing cell division ($n = 3$) were identified during quality control and excluded from quantitative analyses of intracellular fluorescence heterogeneity. All raw single-cell measurements, including these excluded cells, are provided in the deposited dataset. Extreme cells were defined as values lying outside 1.5 times the interquartile range below the first quartile (Q1) or above the third quartile (Q3). Differences in the frequency of extreme cells between diazotrophic and ammonium-replete conditions were evaluated using Fisher's exact test. For Fig. 3c,-d, differences in mean PE fluorescence and coefficients of variation (CV), respectively, were assessed using two-sided *t*-tests. *p*-values <0.05 were considered statistically significant. Nitrogen contents obtained by TEM–EDS (Supporting Information Fig. S2) were compared using *t*-test. Differences in growth rate, Chl *a* content per cell, and POC/PON molar ratios between diazotrophic and ammonium-replete conditions were also assessed using two-sided *t*-tests.

Results

To evaluate whether the two nitrogen-source treatments corresponded to distinct physiological nitrogen states, we measured growth rate, Chl *a* content per cell, POC/PON molar ratios, and N_2 fixation rate (Table 1). Cultures grown with ammonium grew significantly faster and had a higher cellular Chl *a* content compared to diazotrophic cultures (both $p < 0.05$, *t*-test). POC/PON molar ratios were consistently higher under diazotrophy than with ammonium, both at the end of the light and dark periods ($p < 0.05$, *t*-test), indicating a more carbon-rich, nitrogen-limited physiological state under diazotrophy relative to ammonium enrichment. Consistent with the known inhibitory effect of bioavailable dissolved nitrogen on nitrogenase activity, diazotrophic cultures fixed N_2 at a higher cell-specific rate than ammonium-grown cultures. Nonetheless, ammonium-grown cultures continued to fix measurable N_2, suggesting a mixed nitrogen-acquisition strategy rather than a strict metabolic switch (Dekaezemacker and Bonnet 2011; Knapp et al. 2012; Masuda et al. 2013). Together, these data confirm that the two treatments represent physiologically distinct nitrogen states, providing the context needed to interpret PE fluorescence patterns described below.

Table 1. Physiological status of *C. watsonii* PS0609 cultures grown under diazotrophic and ammonium-replete conditions.

	Diazotrophic	With ammonium
Growth rate (d^{-1})	0.12 ± 0.01	0.27 ± 0.01
Chl/cell (pg/cell)	0.25 ± 0.01	0.30 ± 0.02
POC/PON at 12 L (mol/mol)	9.10 ± 0.79	6.78 ± 1.06
POC/PON at 12D (mol/mol)	6.74 ± 0.33	4.72 ± 0.45
N_2 fixation (fmol N/cell/h)	3.28 ± 0.42	1.89 ± 0.43

Three-channel imaging (*see* Fig. 1a–d; Supporting Information Fig. S1) resolved subcellular pigment-protein complexes localization: phycoerythrin (PE) was visualized in red, phycobilisome (PBS) containing allophycocyanin (APC) and/or phycocyanin (PC) in blue, and chlorophyll (Chl) emission mainly from photosystem II (PSII) (hereafter PSII) in green (Fig. 1e–h). RGB overlays enabled co-localization: PSII-coupled PBS lacking PE (PBS_{APC+PC}) appeared cyan, whereas PSII-coupled PE-rich PBS complexes ($PBS_{APC+PC+PE}$) appeared white (color coding in Fig. 1i). The RGB coding also distinguished PSII-uncoupled phycobiliproteins: PE uncoupled from PBS (free-PE) shown in red, and thylakoid membrane uncoupled PBS complexes rich in PE (free-$PBS_{APC+PC+PE}$) shown in magenta (Fig. 1i). Both uncoupled signals localized predominantly to the central part of cells (e.g., Fig. 1b,d; Supporting Information Fig. S1).

Furthermore, the spectral imaging classified individual cells into four distinct types based on the spatial pattern of autofluorescence signal from thylakoids showed in the distribution and spatial co-localization of PE and APC and in the spectral data in the central and peripheral regions (illustrated by lines in Fig. 1e–h). Type 1: cells with APC dominant PE emission in the periphery and with reduced PE + APC emission in the central part; Type 2: cells with similar total intensities of APC and PE emissions (with no effect on APC/PE ratio) throughout the entire cells; Type 3: cells with very high content of PE accompanied by low APC in the central region together with much lower PE content at the cell's periphery; Type 4: cells with PE dominance over APC in both central and peripheral regions (Fig. 1e–h).

The three channels imaging setup was then used to observe the effect of nitrogen source on allocation of PE, APC, and PSII based on Chl emission (Fig. 2; Supporting Information Fig. S1). Under diazotrophy, cells often exhibited central PSII-uncoupled PE fluorescence (free-PE; red) and peripheral PBS containing either with (magenta) or without PE (cyan), co-localized with thylakoid membranes (Masuda et al. 2022) (Fig. 2a,c; Supporting Information Fig. S1), both day and night. With ammonium, the distribution pattern shifted: at night, PSII-coupled, PE-absent PBS (PBS_{APC+PC}; cyan) were restricted to the cell periphery near the cell membrane, alongside PE-rich PBS (free-$PBS_{APC+PC+PE}$; magenta), while the center lacked pigment-protein complexes (Fig. 2b). In contrast, during the daytime, the periphery was dominated either by PE-lacking PBS (PSII-PBS_{APC+PC}; cyan) or PSII-uncoupled PE-rich PBS (free-$PBS_{APC+PC+PE}$; magenta). Across conditions and

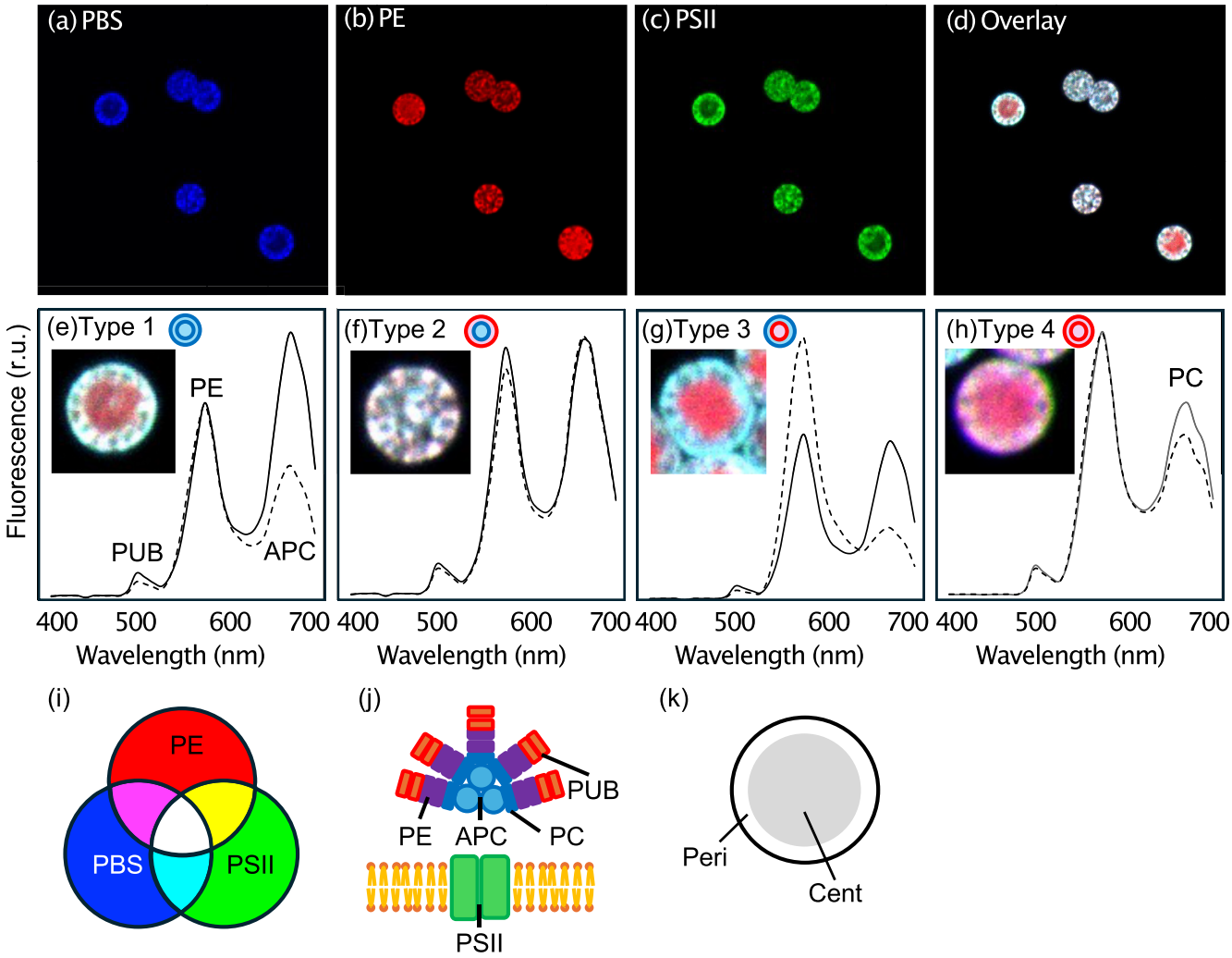

Fig. 1. Typical three layers imaging of (**a**) phycobilisome (PBS), (**b**) phycoerythrin (PE) and (**c**) photosystem II (PSII), and (**d**) overlay of (a–c) in *C. watsonii* PS0609. (**e**–**h**) Cellular types based on the relationship between 488 nm excited PE and allophycocyanin (APC) fluorescence in *C. watsonii* PS0609. We defined four types of cells based on the relationship between PE and APC observed by spectral imaging. Black lines in (e–h) show emission spectra of peripheric part and dotted lines of centric part of the cells. The peaks of PUB, PE, PC, and APC emission were 504, 575, 656, and 664 nm, respectively. We note that PBS includes PBS with PE ($PBS_{APC+PC+PE}$) and PBS without PE (PBS_{APC+PC}). Co-localization of pigment-protein complexes based on three-layer images in (e–h) shows the coupling status of PE (red) for PBS (blue), and PSII coupled to PSII (green). Color codes and schematic view of relationship among PE, PBS, and PSII are found in (**i**) and (**j**), respectively. The RGB combinations then represented the color code for coupling status. The cell areas with PBS without PE (PBS_{APC+PC}) coupled to PSII found as cyan and areas with PBS rich in PE ($PBS_{APC+PC+PE}$) coupled to PSII shown as white. PE uncoupled from PBS (free-PE) is present in red and uncoupled PBS containing PE, PC and APC (free-$PBS_{APC+PC+PE}$) is shown as magenta. (**k**) Schematic view of peripheric and central part of the cell. PSII, photosystem II; APC, allophycocyanin; PC, phycocyanin; PE, phycoerythrin; PUB, phycourobilin; Cent, central part of the cell; Peri, peripheral part of the cell.

photoperiods, discrete white hotspots—PSII-coupled, PE-rich PBS (PSII-$PBS_{APC+PC+PE}$)—were present at the cell periphery showing cell-to-cell heterogeneity. In addition, there was intracellular spatial heterogeneity in membrane microdomains visible as different colors alongside the thylakoid membrane of single cells. Specifically, we were able to detect white hotspots containing PSII-coupled PE-rich PBSs (under both diazotrophic and non-diazotrophic conditions) and more continuous membrane areas often with PSII-coupled PE-lacking PBSs (Fig. 2).

To quantify the diel changes in PE localization outside of thylakoid membrane, we analyzed the PE fluorescence in the central region of the cells (Fig. 3a–c). The mean fluorescence intensity ranged from 30 to 40 (r. u.), with individual cell values varying from 15 to 152 (r. u.). Notably, cells exhibiting high fluorescence—hereafter referred to as "extreme cells"—were more frequently observed during the daytime and significantly more numerous under diazotrophy (Fig. 3a) than with ammonium (N_2: 110/1488 cells, 7.39%; NH_4^+: 7/607 cells, 1.15%; Fisher's exact test, $p < 0.001$) (Figs. 2c and 3b). Elevated

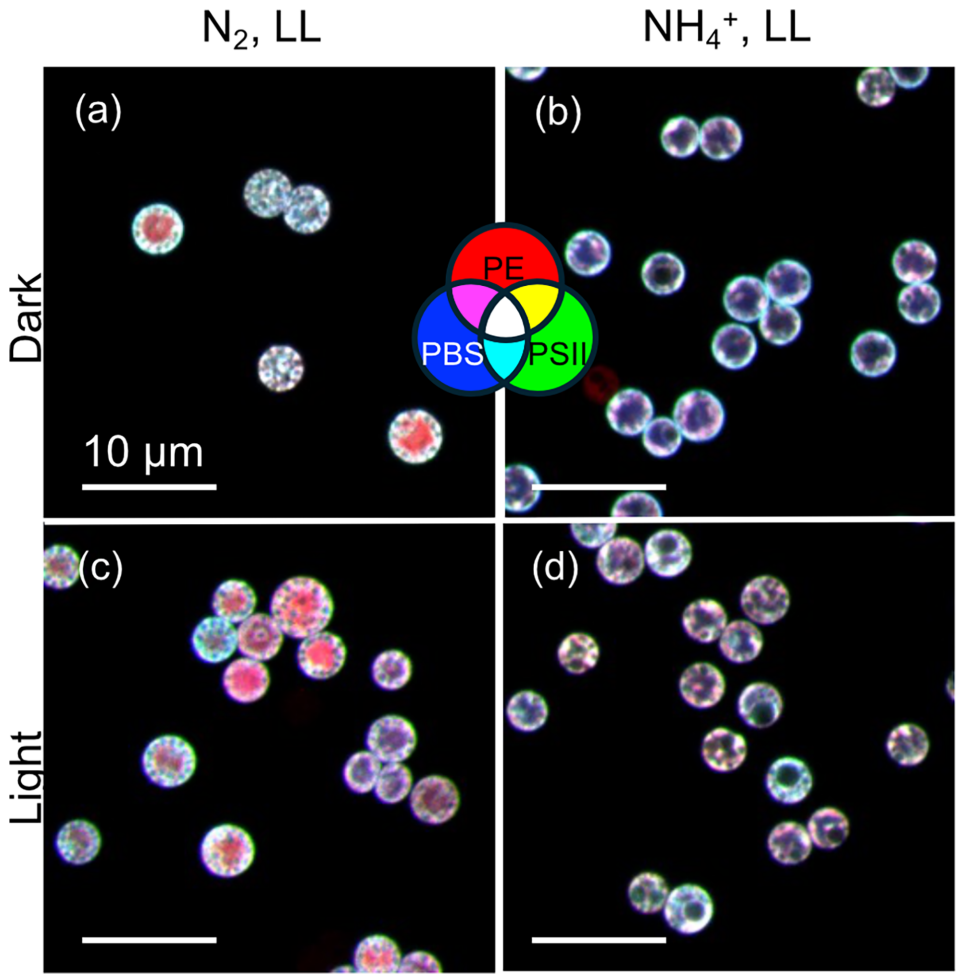

Fig. 2. Typical co-localization of pigment-protein complexes in *C. watsonii* PS0609. Cells were grown at light/dark diel cycle (12 h/12 h) and imaged at different time-spots (6 h in the dark, **a** and **b**; 6 h in the light, **c** and **d**). Cells were grown either in diazotrophic conditions (a, c), or grown in the presence of NH_4^+ (b, d). Three channel RGB pictures represent acquired fluorescence signals showing localization of three pigment–proteins: PE (red), PBS (blue), and Chl emission from PSII (green). Total number of analyzed cells per each condition was between 58 and 255. Color codes follow Fig. 1.

central PE fluorescence likely reflects either an increased number of PE uncoupled from PBS (red in Supporting Information Fig. S1) or free PE rich $PBS_{APC+PC+PE}$, uncoupled from PSII (magenta in Supporting Information Fig. S1).

With ammonium, central PE fluorescence was lower than under diazotrophy ($p < 0.001$, *t*-test) (Fig. 3c) consistent with PE being generally PBS-associated at peripheral thylakoids (Supporting Information Fig. S2a,b). Under diazotrophy, PE intracellular heterogeneity evaluated as coefficient of variation (CV) was higher in the center than in the periphery ($p < 0.001$; Fig. 3d), indicating that central thylakoid architecture shapes intracellular variability. In contrast, such a spatial difference in CV was markedly reduced, and no strong center-dominated heterogeneity was observed under ammonium-replete conditions (Fig. 3d). The TEM–EDS analysis of *C. watsonii* WH8501 showed no significant difference in nitrogen content (as percentage of C, N, O and P) between central and peripheral region during the dark (Supporting Information Fig. S2), with nitrogen content in the central region tending to be higher by day ($p > 0.05$; Supporting Information Fig. S2).

Time-series analysis showed clear diel changes in cell-types' composition (Fig. 4). Under diazotrophy, Type 3 cells (PE-rich center) account for 30–68% of the population during the dark period. Proportion of Type 4 cells (PE dominant throughout) increased from mid dark through mid-light, peaking at 95% at 3 h after lights-on, then declined toward the end of the photoperiod as Type 3 rose just before the onset of darkness. Proportion of Type 1 cells (APC-dominant throughout) reached 32% 1 h after lights-off. Proportion of Type 2 cells (peripheral PE only) remained a minor population (< 2.2%) throughout the cycle (Fig. 4). Similar trend was shown from the cells grown under higher light intensity (Fig. 4).

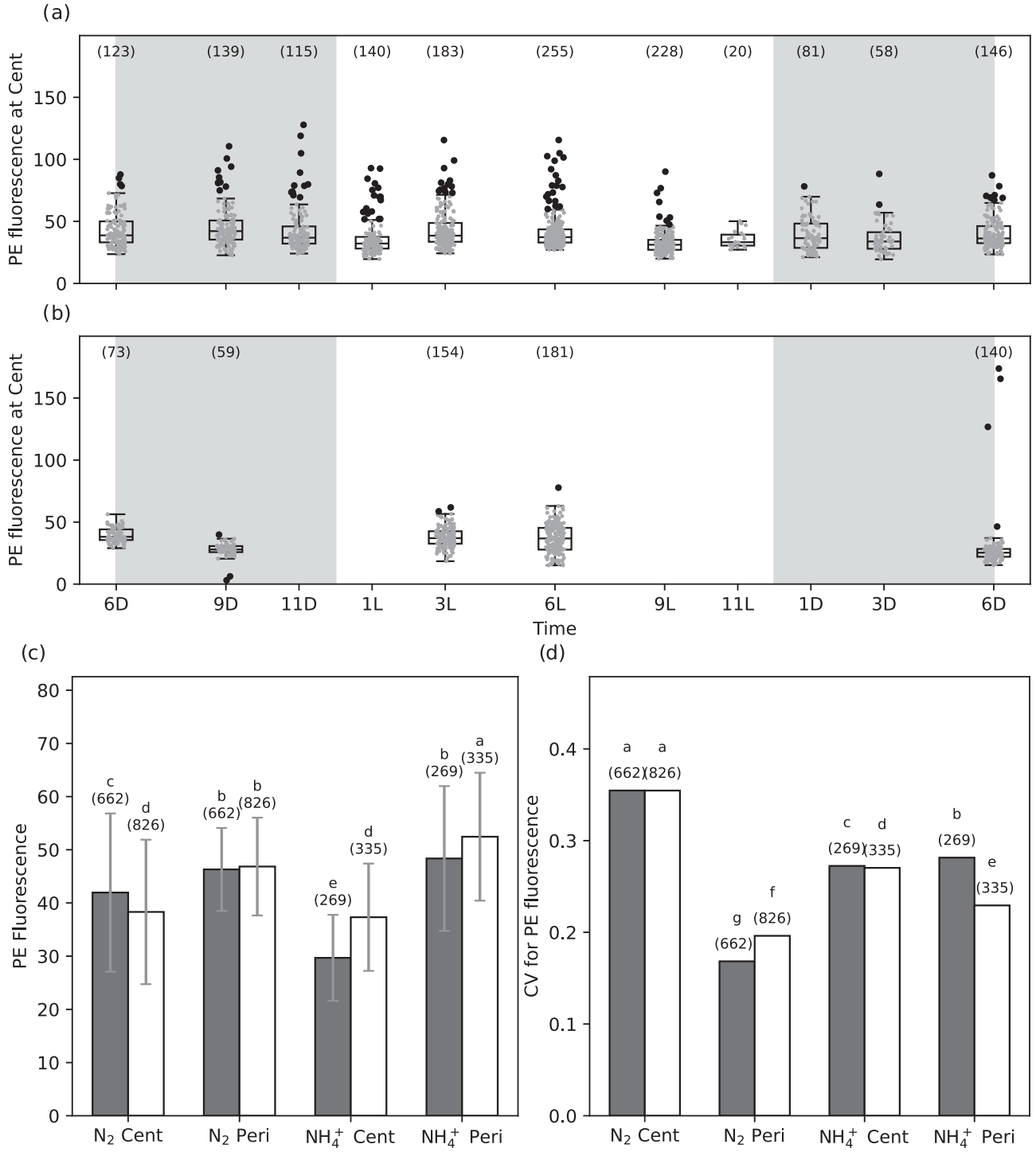

Fig. 3. Temporal changes in PE fluorescence during the diel cycle. Temporal changes of PE fluorescence in the central part (Cent) for (**a**) cells under N_2 fixing conditions and (**b**) cells with NH_4^+ available. Gray dots represent data obtained from individual cells, and black dots represent outliers. Outliers are defined as outside 1.5 times the interquartile range above the upper quartile and below the lower quartile. The dark periods are indicated by shadows. (**c**) Mean PE fluorescence intensity (± standard deviation) in the central (Cent) and peripheral (Peri) regions during dark (black bars) and light (white bars) periods. Numbers in parentheses indicate the number of cells analyzed. (**d**) Intracellular heterogeneity of PE fluorescence, expressed as the coefficient of variation (CV), in the central and peripheral regions during dark and light periods. CV values were calculated from raw single-cell fluorescence measurements. Statistical significance in panels (c) and (d) was assessed using *t*-test. Different letters above bars indicate statistically significant differences after correction for multiple comparisons ($p < 0.05$). PE, phycoerythrin; Cent, central region; Peri, Peripheric region; N_2, diazotrophic; NH_4^+, ammonium available condition.

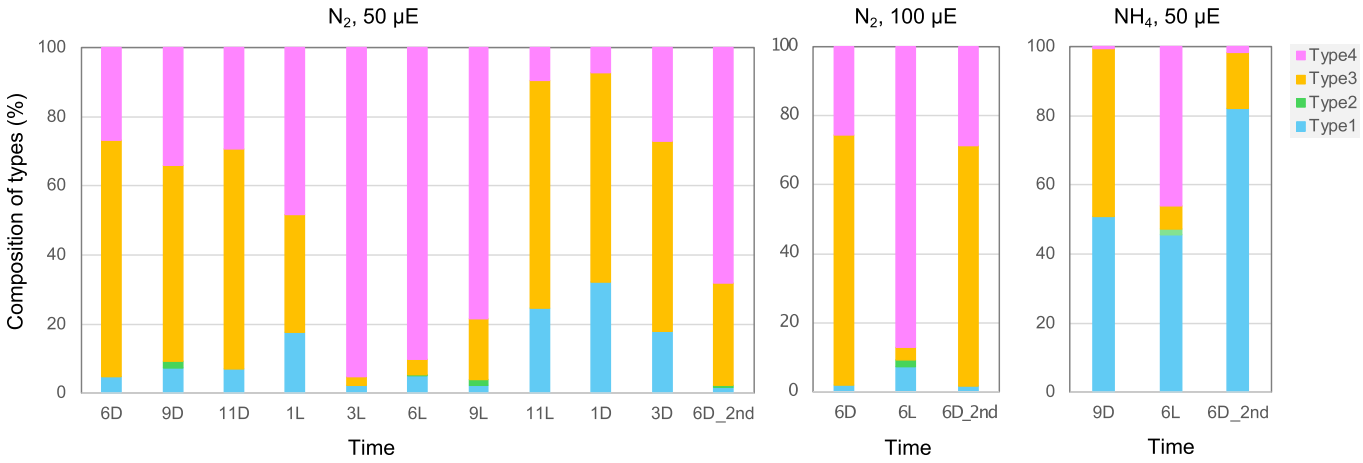

Fig. 4. Temporal changes of four defined cell spectral types (Fig. 1). Under diazotrophy, a clear temporal shift, with Type 3 cells dominant in the dark phase and Type 4 cells dominant in the light phase, was observed. Type 1 cells (APC dominant) also showed a transient peak early in the dark phase. With ammonium, Type 1 cells were more abundant, while Type 3 dominated in the dark and Type 4 in the light.

With ammonium, the proportion of Type 1 cells remained consistently higher than under diazotrophy (46–82%). As in diazotrophy, Type 3 cells predominated at night and Type 4 by day. These patterns suggest nightly disassembly and central redistribution of peripheral, PBS-associated PE, followed by daytime reassembly at the periphery (Fig. 4). We note that the 2nd 6 h in the dark ("6D_2nd") differed from the first dark phase, likely reflecting day-to-day variability in population structure associated with the slow growth rate of *C. watsonii*.

Discussion

Three-channel imaging distinguished PSII, different types of PBS ($PBS_{APC+PC+PE}$ and PBS_{APC+PC}) and free PE's allowing us to map their co-localization at the cell periphery vs. center. Under diazotrophic conditions, a variable proportion of PE was uncoupled from photosynthetic energy transfer and localized centrally as either (i) free PE fully detached from PBS complex (red) or (ii) PE-rich PBS ($PBS_{APC+PC+PE}$) decoupled from PBII (magenta) (Figs. 1 and 2; Supporting Information Fig. S1). In contrast, with ammonium, free-PE was rarely observed; PE remained PSII-coupled within peripheral membrane microdomains (white), and central red/magenta signals were largely absent. Non-diazotrophic cells also showed more PSII-coupled PBS microdomains at night but still lacked central free-PE or PE-rich PBS (Figs. 1 and 2; Supporting Information Fig. S1). These patterns differ from those of *Synechococcus* DC2, where the fraction of PE-absorbed light decreased as autofluorescence increases under nitrogen-replete conditions (Wyman et al. 1985). In *C. watsonii*, nitrogen-repletion instead coincides with the loss of free-PE and retention of PSII-coupled PE in peripheral hotspots whereas diazotrophy promotes central PE uncoupling. We therefore suggest that uncoupled free-PE or PE bound to uncoupled PBS has a non-light-harvesting role, potentially linked to N_2 fixation. Consistent with this view, diazotrophic conditions produced "extreme" PE-bright cells despite similar mean PE fluorescence across the diel cycle (Fig. 3). Because PE fluorescence was measured using 488 nm excitation, which directly excites both PE and chlorophyll (490–606 nm emission), the resulting spectra integrate direct excitation with energy-transfer contributions and thus reflect the photophysical and coupling state of PE rather than its absolute abundance. Consequently, PE–PBS–PSII coupling relationships cannot be uniquely resolved from these spectra and should be interpreted as a range of configurations consistent with the observed spectral types—meaning that similar mean PE fluorescence does not exclude substantial differences in PE allocation or function between treatments. Together with PE's classic role in light-harvesting (French and Young 1952), chromatic adaptation (Anderson and Grossman 1990) and photoprotection (Kaňa et al. 2012; Tamary et al. 2012), our observations support an additional function of PE in *C. watsonii*. We speculate that PE accumulation in the central part of nitrogen-fixing cells may act as a temporary sink for assimilated nitrogen during periods of active N_2 fixation.

These physiological differences confirm a nitrogen-replete state under ammonium enrichment, yet *C. watsonii* continued to fix N_2 in its presence (Table 1). Phycobiliproteins more broadly act as dynamic nitrogen reservoirs not necessarily scaling with bulk cellular nitrogen (Yamanaka and Glazer 1980; Wyman et al. 1985), and carbon/nitrogen uptake in *C. watsonii* can be decoupled at the single-cell level, masking metabolic heterogeneity in population-averaged signals (Masuda et al. 2020; Polerecky et al. 2021).

Under diazotrophy, three-channel imaging showed intracellular accumulation and diel relocation of free PE relative to PBS-coupled PE in *C. watsonii* (Figs. 2a,c, 3, and 4): central

free-PE was prominent at night when N_2 fixation peaks, whereas under ammonium, free PE was largely absent and PE remained PSII coupled in peripheral microdomains (Fig. 2), indicating tight linkage to cellular nitrogen status. These findings are consistent with earlier studies showing nitrogen starvation–induced PE degradation in non-diazotrophic cyanobacteria, such as *Synechococcus*, where PE breakdown supports nitrogen homeostasis (Yamanaka and Glazer 1980; Wyman et al. 1985; Jörg et al. 2001) and also in PE containing cryptophytes (Christiane 1980; Rhiel et al. 1986; Silva et al. 2009). Since PE can constitute ~20% of cellular protein (Rodriguez et al. 1989), shifts in its state and distribution can directly influence cellular nitrogen allocation; yet bulk elemental N distribution (as a fraction of total C, N, O and P content as determined by electron microscopy/Energy Dispersive Spectroscopy; *see* Supporting Information Fig. S2) did not differ between diazotrophic and ammonium treatments in WH8501 (Supporting Information Fig. S2), suggesting functional redistribution rather than a change in pool size. Cyanophycin production in PE-rich *Synechococcus* (Wingard et al. 2002) and in *C. watsonii* (Mohr et al. 2010) further supports a general strategy of leveraging phycobiliproteins as a transient buffer. Finally, the diel oscillation in PE status (Free- or PBS-coupled), content, and localization implies co-regulation by light and nitrogen availability, consistent with transcriptional control of phycobiliproteins by both cues (Liotenberg et al. 1996). Together, these observations support a dual role for PE in *C. watsonii*—as a light-harvesting pigment and temporally regulated nitrogen reservoir that facilitates efficient N_2 fixation.

Under diazotrophic conditions, three-channel imaging revealed marked cell-to-cell heterogeneity in the function of photosynthesis-related proteins (Fig. 2; Supporting Information Fig. S1). PE in the central part of the cells were dominantly independent of PBS (red in Supporting Information Fig. S1), consistent with PE disassembled from PBS rather than de novo synthesis, because PE biosynthesis occurs within PBS (Stadnichuk et al. 2015). In some cells, the complete PE-containing PBS complexes ($PBS_{APC+PC+PE}$) remained peripheral (magenta in Supporting Information Fig. S1). Similar PBS dissociation and energetic decoupling from PSII have been documented in *Synechococcus* (Moore et al. 2020) and tied to specific physiological roles (Kaňa et al. 2012; Tamary et al. 2012). In addition, PE decoupling has been linked to nitrogen assimilation at single-cell and at subcellular scales in *Trichodesmium* (Berman-Frank et al. 2001). Although we did not trace colony dynamics, *C. watsonii* often forms colonies (Foster et al. 2013; Mohr et al. 2013), which may facilitate nitrogen transfer and communal energy management (Masuda et al. 2020), offering a plausible basis for observed cell-to-cell heterogeneity in PE fluorescence.

Cell-to-cell heterogeneity among single cells has recently been reported to be a common phenomenon in single-cell organisms, including fungi, bacteria, and cyanobacteria (Ackermann 2015; van Boxtel et al. 2017; Kaňa et al. 2024). In cyanobacteria, the cell-to-cell phenotypic heterogeneity has been reported for nitrogen fixation (Foster et al. 2013; Mohr et al. 2013; Masuda et al. 2020), cell size (Martins et al. 2018), photodamage responses (Tay and Cameron 2023), carbon and nitrogen allocation (Polerecky et al. 2021), and the location and dynamics of photosynthesis-related proteins—including membrane microdomains and colony-associated fluorescence (Kaňa et al. 2024). Proposed drivers of the variation include stochastic gene expression and partitioning at cell division, as well as the cell cycle and its interaction with the circadian clock (Ackermann 2015; Martins et al. 2018). Given the reported cell-to-cell heterogeneity in N_2 fixation activity, it is conceivable that, in *C. watsonii*, the cellular amount and/or state of free PE may be linked to N_2 fixation. However, this possible relationship remains speculative and will require direct experimental validation.

In addition to cell-to-cell heterogeneity, we observed subcellular heterogeneity: PSII-coupled, PE-rich PBS hotspots appeared as discrete peripheral hotspots (white; Fig. 2). Such subcellular spatial heterogeneity is consistent with proteins and lipid nano/microdomains in cyanobacteria (Johnson et al. 2014; Koochak et al. 2019; Straskova et al. 2019) and with the reported PSI, PSII and PBS allocation dynamics in *Synechocystis*, *Synechococcus* and *Trichodesmium* (Konert et al. 2019; Straskova et al. 2019).

Author Contributions

Takako Masuda, Radek Kaňa, and Ondřej Prásil designed the experiments. Takako Masuda and Grzegorz Konert carried out the experiment and analyzed data supervised by Radek Kaňa and Ondřej Prásil. Takako Masuda shaped the concept of the study, and Grzegorz Konert developed the image analysis. Marie Vancová, Dominik Pinkas, and Vlada Filimonenko conducted TEM and EDS analysis. Takako Masuda wrote the original draft with substantial input from all the authors.

Acknowledgments

The authors thank Olexandra Demianyk, Barbora Šedivá and Jiri Šetlík at Center Algatech for excellent technical assistance. This research was supported by GAČR (project 23-06593S to Ondřej Prásil) and by OP JAK project "Photomachines" (Reg. No. CZ.02.01.01/00/22_008/0004624), JST PRESTO (JPMJPR23GA), JSPS KAKENHI (23H02301). We acknowledge the Biology Center Czech Academy of Sciences core facility laboratory of Electron Microscopy and the Electron Microscopy Core Facility at the Institute of Molecular Genetics, Prague, Czech Republic, supported by MEYS (LM2023050) and ERDF (CZ.02.1.01/0.0/0.0/18_046/0016045, CZ.02.01.01/00/23_015/0008205) for their support with

obtaining the electron microscopy and EDS data presented herein.

Conflicts of Interest

None declared.

Data Availability Statement

All the data used to generate the graphs presented in the figures can be found at https://doi.org/10.5281/zenodo.21250576.

References

Ackermann, M. 2015. "A Functional Perspective on Phenotypic Heterogeneity in Microorganisms." *Nature Reviews. Microbiology* 13: 497–508. https://doi.org/10.1038/nrmicro3491.

Anderson, L. K., and A. R. Grossman. 1990. "Structure and Light-Regulated Expression of Phycoerythrin Genes in Wild-Type and Phycobilisome Assembly Mutants of *Synechocystis* Sp. Strain PCC 6701." *Journal of Bacteriology* 172: 1297–1305. https://doi.org/10.1128/jb.172.3.1297-1305.1990.

Bell, P. R. F., and F.-X. Fu. 2005. "Effect of Light on Growth, Pigmentation and N_2 Fixation of Cultured *Trichodesmium* Sp. From the Great Barrier Reef Lagoon." *Hydrobiologia* 543: 25–35. https://doi.org/10.1007/s10750-004-5713-2.

Berman-Frank, I., P. Lundgren, Y. B. Chen, et al. 2001. "Segregation of Nitrogen Fixation and Oxygenic Photosynthesis in the Marine Cyanobacterium Trichodesmium." *Science* 294, no. 5546: 1534–1537.

Chen, Y., J. P. Zehr, and M. Mellon. 1996. "Growth and Nitrogen Fixation of the Diazotrophic Filamentous Nonheterocystous Cyanobacterium *Trichodesmium* Sp. IMS 101 in Defined Media: Evidence for a Circadian Rhythm." *Journal of Phycology* 32: 916–923. https://doi.org/10.1111/j.0022-3646.1996.00916.x.

Christiane, L. 1980. "Effects if Butrigeb Deficiency and Light of High Intensity of Crypromonas Refescens (Criptophyceae)." *Protoplasma* 102: 11–19.

Dekaezemacker, J., and S. Bonnet. 2011. "Sensitivity of N_2 Fixation to Combined Nitrogen Forms (NO_3^- and NH_4^+) in Two Strains of the Marine Diazotroph *Crocosphaera watsonii* (Cyanobacteria)." *Marine Ecology Progress Series* 438: 33–46. https://doi.org/10.3354/meps.

Dron, A., S. Rabouille, P. Claquin, B. Le Roy, A. Talec, and A. Sciandra. 2012. "Light–Dark (12 : 12) Cycle of Carbon and Nitrogen Metabolism in *Crocosphaera watsonii* WH8501: Relation to the Cell Cycle." *Environmental Microbiology* 14: 967–981. https://doi.org/10.1111/j.1462-2920.2011.02675.x.

Foster, R. A., S. Sztejrenszus, and M. M. Kuypers. 2013. "Measuring Carbon and N_2 Fixation in Field Populations of Colonial and Free-Living Unicellular Cyanobacteria Using Nanometer-Scale Secondary Ion Mass Spectrometry." *Journal of Phycology* 49: 502–516. https://doi.org/10.1111/jpy.12057.

French, C. S., and V. K. Young. 1952. "The Fluorescence Spectra of Red Algae and the Transfer of Energy From Phycoerythrin to Phycocyanin and Chlorophyll." *The Journal of General Physiology* 35: 873–890. https://doi.org/10.1085/jgp.35.6.873.

Fujita, Y., and S. Shimura. 1974. "Phycoerythrin of the Marine Blue-Algae *Trichodesmium thiebautii*." *Plant and Cell Physiology* 15: 939–942. https://doi.org/10.1007/BF00391624.

Gruber, N., and J. N. Galloway. 2008. "An Earth-System Perspective of the Global Nitrogen Cycle." *Nature* 451: 293–296. https://doi.org/10.1038/nature06592.

Johnson, M. P., C. Vasilev, J. D. Olsen, and C. N. Hunter. 2014. "Nanodomains of Cytochrome b6f and Photosystem II Complexes in Spinach Grana Thylakoid Membranes." *Plant Cell* 26: 3051–3061. https://doi.org/10.1105/tpc.114.127233.

Jörg, S., S. Ulrich, S. Roland, V. Uwe, and F. Karl. 2001. "Nitrogen Starvation-Induced Chlorosis in Synechococcus PCC 7942. Low-Level Photosynthesis as a Mechanism of Long-Term Survival." *Plant Physiology* 126, no. 1: 233–243.

Kaňa, R., M. Eichner, A. Gall, and C. Ilioaia. 2024. "Spatial Heterogeneity in the Photobiology of Phototrophs—Questions and Methods." *Frontiers in Photobiology* 2: 01–13. https://doi.org/10.3389/fphbi.2024.1384522.

Kaňa, R., E. Kotabová, O. Komárek, et al. 2012. "The Slow S to M Fluorescence Rise in Cyanobacteria Is Due to a State 2 to State 1 Transition." *Biochimica et Biophysica Acta* 1817: 1237–1247. https://doi.org/10.1016/j.bbabio.2012.02.024.

Knapp, A. N., J. Dekaezemacker, S. Bonnet, J. A. Sohm, and D. G. Capone. 2012. "Sensitivity of *Trichodesmium erythraeum* and *Crocosphaera watsonii* Abundance and N_2 Fixation Rates to Varying NO_3^- and PO_4^{3-} Concentrations in Batch Cultures." *Aquatic Microbial Ecology* 66: 223–236. https://doi.org/10.3354/ame01577.

Konert, G., G. Steinbach, M. Canonico, and R. Kaňa. 2019. "Protein Arrangement Factor: A New Photosynthetic Parameter Characterising the Organisation of Thylakoid Membrane Proteins." *Physiologia Plantarum* 166: 264–277. https://doi.org/10.1111/ppl.12952.

Koochak, H., S. Puthiyaveetil, D. L. Mullendore, M. Li, and H. Kirchhoff. 2019. "The Structural and Functional Domains of Plant Thylakoid Membranes." *The Plant Journal* 97: 412–429. https://doi.org/10.1111/tpj.14127.

Liotenberg, S., D. Campbell, R. Rippka, J. Houmard, and N. Tandeau de Marsac. 1996. "Effect of the Nitrogen Source on Phycobiliprotein Synthesis and Cell Reserves in a Chromatically Adapting Filamentous Cyanobacterium." *Microbiology* 142: 611–622.

Martins, B. M. C., A. K. Tooke, P. Thomas, and J. C. W. Locke. 2018. "Cell Size Control Driven by the Circadian Clock and Environment in Cyanobacteria." *Proceedings of the National*

Academy of Sciences of the United States of America 115: E11415–E11424. https://doi.org/10.1073/pnas.1811309115.

Masuda, T., K. Furuya, T. Kodama, S. Takeda, and P. J. Harrison. 2013. "Ammonium Uptake and Dinitrogen Fixation by the Unicellular Nanocyanobacterium *Crocosphaera watsonii* in Nitrogen-Limited Continuous Cultures." *Limnology and Oceanography* 58: 2029–2036. https://doi.org/10.4319/lo.2013.58.6.2029.

Masuda, T., K. Inomura, J. Mares, and O. Prasil. 2022. "Crocosphaera Watsonii." *Trends in Microbiology* 30: 805–806. https://doi.org/10.1016/j.tim.2022.02.006.

Masuda, T., K. Inomura, N. Takahata, et al. 2020. "Heterogeneous N_2 Fixation Rates Confer Energetic Advantage and Expanded Ecological Niche of Unicellular Diazotroph Populations." *Communications Biology* 3: 172. https://doi.org/10.1038/s42003-020-0894-4.

Masuda, T., J. Mares, T. Shiozaki, K. Inomura, A. Fujiwara, and O. Prasil. 2024. "*Crocosphaera watsonii*—A Widespread Nitrogen-Fixing Unicellular Marine Cyanobacterium." *Journal of Phycology* 60: 604–620. https://doi.org/10.1111/jpy.13450.

Mohr, W., M. P. Intermaggio, and J. LaRoche. 2010. "Diel Rhythm of Nitrogen and Carbon Metabolism in the Unicellular, Diazotrophic Cyanobacterium Crocosphaera Watsonii WH8501." *Environmental Microbiology* 12, no. 2: 412–421.

Mohr, W., T. Vagner, M. M. Kuypers, M. Ackermann, and J. La Roche. 2013. "Resolution of Conflicting Signals at the Single-Cell Level in the Regulation of Cyanobacterial Photosynthesis and Nitrogen Fixation." *PLoS One* 8: e66060. https://doi.org/10.1371/journal.pone.0066060.

Montoya, J. P., C. M. Holl, J. P. Zehr, A. Hansen, T. A. Villareal, and D. G. Capone. 2004. "High Rates of N_2 Fixation by Unicellular Diazotrophs in the Oligotrophic Pacific Ocean." *Nature* 430: 1027–1032. https://doi.org/10.1038/nature02824.

Montoya, J. P., M. Voss, P. Kaehler, and D. G. Capone. 1996. "A Simple, High Precision, High Sensitivity Tracer Assay for Dinitrogen Fixation." *Applied and Environmental Microbiology* 62: 986–993. https://doi.org/10.1128/aem.62.3.986-993.1996.

Moore, K. A., S. Altus, J. W. Tay, et al. 2020. "Mechanical Regulation of Photosynthesis in Cyanobacteria." *Nature Microbiology* 5: 757–767.

Mulholland, M. R., D. A. Bronk, and D. G. Capone. 2004. "Dinitrogen Fixation and Release of Ammonium and Dissolved Organic Nitrogen by Trichodesmium IMS101." *Aquatic Microbial Ecology* 37: 85–94. https://doi.org/10.3354/ame037085.

Neveux, J., F. Lantoine, D. Vaulot, D. Marie, and J. Blanchot. 1999. "Phycoerythrins in the Southern Tropical and Equatorial Pacific Ocean: Evidence for New Cyanobacterial Types." *Journal of Geophysical Research* 104: 3311–3321. https://doi.org/10.1029/98JC02000.

Polerecky, L., T. Masuda, M. Eichner, et al. 2021. "Temporal Patterns and Intra- and Inter-Cellular Variability in Carbon and Nitrogen Assimilation by the Unicellular Cyanobacterium *Cyanothece* Sp. ATCC 51142." *Frontiers in Microbiology* 12: 620915. https://doi.org/10.3389/fmicb.2021.620915.

Porra, R. J., W. A. Thompson, and P. E. Kriedemann. 1989. "Determination of Accurate Extinction Coefficients and Simultaneous Equations for Assaying Chlorophylls *a* and *b* Extracted with Four Different Solvents: Verification of the Concentration of Chlorophyll Standards by Atomic Absorption Spectroscopy." *Biochimica et Biophysica Acta, Bioenergetics* 975: 384–394. https://doi.org/10.1016/S0005-2728(89)80347-0.

Rhiel, E., K. Krupinska, and W. Whehrmeyer. 1986. "Effects on Nitrogen Starvation on the Function and Organization of the Photosynthetic Membranes in Crypromonas Maculata (Cryptophyceae)." *Planta* 169: 361–369.

Rodriguez, H., J. Rivas, M. G. Guerrero, and M. Losada. 1989. "Nitrogen-Fixing Cyanobacterium with High Phycoerythrin Content." *Applied and Environmental Microbiology* 55, no. 3: 758–760.

Shi, T., I. Ilikchyan, S. Rabouille, and J. P. Zehr. 2010. "Genome-Wide Analysis of Diel Gene Expression in the Unicellular N_2-Fixing Cyanobacterium *Crocosphaera watsonii* WH 8501." *The ISME Journal* 4: 621–632. https://doi.org/10.1038/ismej.2009.148.

Shiozaki, T., M. Ijichi, T. Kodama, S. Takeda, and K. Furuya. 2014. "Heterotrophic Bacteria as Major Nitrogen Fixers in the Euphotic Zone of the Indian Ocean." *Global Biogeochemical Cycles* 28: 1096–1110. https://doi.org/10.1002/2014gb004886.

Silva, A. F., S. O. Lourenco, and R. M. Chaloub. 2009. "Effects of Nitrogen Starvation on the Photosynthetic Physiology of a Tropical Marine Microalga Rhodomonas Sp. (Cryptophyceae)." *Aquatic Botany* 91, no. 4: 291–297.

Stadnichuk, I. N., P. M. Krasilnikov, and D. V. Zlenko. 2015. "Cyanobacterial Phycobilisomes and Phycobiliproteins." *Microbiology* 84, no. 2: 101–111.

Straskova, A., G. Steinbach, G. Konert, et al. 2019. "Pigment–Protein Complexes Are Organized into Stable Microdomains in Cyanobacterial Thylakoids." *Biochimica et Biophysica Acta, Bioenergetics* 1860: 148053. https://doi.org/10.1016/j.bbabio.2019.07.008.

Swanson, R. V., L. J. Ong, S. M. Wilbanks, and A. N. Glazer. 1991. "Phycoerythrins of Marine Unicellular Cyanobacteria. II. Characterization of Phycobiliproteins with Unusually High Phycourobilin Content." *The Journal of Biological Chemistry* 266: 9528–9534. https://doi.org/10.1016/S0021-9258(18)92852-8.

Tamary, E., V. Kiss, R. Nevo, et al. 2012. "Structural and Functional Alterations of Cyanobacterial Phycobilisomes Induced by High-Light Stress." *Biochimica et Biophysica Acta* 1817: 319–327. https://doi.org/10.1016/j.bbabio.2011.11.008.

Tay, J. W., and J. C. Cameron. 2023. "Asymmetric Survival in Single-Cell Lineages of Cyanobacteria in Response to Photodamage." *Photosynthesis Research* 155: 289–297. https://doi.org/10.1007/s11120-022-00986-9.

van Boxtel, C., J. H. van Heerden, N. Nordholt, P. Schmidt, and F. J. Bruggeman. 2017. "Taking Chances and Making Mistakes: Non-Genetic Phenotypic Heterogeneity and Its Consequences for Surviving in Dynamic Environments." *Journal of the Royal Society Interface* 14: 20170141. https://doi.org/10.1098/rsif.2017.0141.

Wingard, L. L., S. R. Miller, J. M. Sellker, E. Stenn, M. M. Allen, and A. M. Wood. 2002. "Cyanophycin Production in a Phycoerythrin-Containing Marine Synechococcus Strain of Unusual Phylogenetic Affinity." *Applied and Environmental Microbiology* 68, no. 4: 1772–1777.

Wyman, M., R. P. F. Gregory, and N. G. Carr. 1985. "Novel Role for Phycoerythrin in a Marine Cyanobacterium, *Synechococcus* StrainDC2." *Science* 230: 818–820. https://doi.org/10.1126/science.230.4727.818.

Yamanaka, G., and A. N. Glazer. 1980. "Dynamic Aspects of Phycobilisome Structure. Phycobilisome Turnover during Nitrogen Starvation in *Synechococcus* Sp." *Archives of Microbiology* 124: 39–47. https://doi.org/10.1007/BF00407026.

Zehr, J. P., M. T. Mellon, and S. Zani. 1998. "New Nitrogen Fixing Microorganisms Detected in Oligotrophic Oceans by the Amplification of Nitrogenase (*nifH*) Genes." *Applied and Environmental Microbiology* 64: 3444–3450. https://doi.org/10.1128/AEM.

Zehr, J. P., J. B. Waterbury, P. J. Turner, et al. 2001. "Unicellular Cyanobacteria Fix N_2 in the Subtropical North Pacifc Ocean." *Nature* 412: 635–638. https://doi.org/10.1038/35088063.

Supporting Information

Additional Supporting Information may be found in the online version of this article.

Submitted 31 October 2025
Revised 13 August 2026
Accepted 17 August 2026